

Submitted as v2 to arXiv.org April 19, 2019

Universal constants and equations of turbulent motion

by Helmut Z. Baumert,

Institute for Applied Marine and Limnic Studies (IAMARIS e.V.), Hamburg, Germany

Abstract. In the spirit of Prandtl’s [1926] conjecture, for turbulence at $Re \rightarrow \infty$ we present an analogy with the kinetic theory of gases, with dipoles made of quasi-rigid and “dressed” vortex tubes as frictionless, incompressible but deformable quasi-particles. Their movements are governed by Helmholtz’ elementary vortex rules applied locally. A contact interaction or “collision” leads either to random scatter of a trajectory or to the formation of two likewise rotating, fundamentally unstable whirls forming a dissipative patch slowly rotating around its center of mass which is almost at rest. This approach predicts von Karman’s constant as $\kappa = 1/\sqrt{2\pi} \simeq 0.399$ and the spatio-temporal dynamics of energy-containing time and length scales controlling turbulent mixing [Baumert, 2009] in agreement with observations. A link to turbulence spectra was missing so far. In the present paper it is shown that the above image of random vortex-dipole movements is compatible with Kolmogorov’s turbulence spectra if dissipative patches, beginning as two *likewise* rotating eddies, evolve locally into a space-filling bearing in the sense of Herrmann [1990], i.e. into an “Apollonian gear” consisting of incompressible and flexibly deformable vortex tubes which are frictionless, excepting the dissipative scale of size zero.

For steady and locally homogeneous conditions our approach predicts the pre-factor in the three-dimensional Eulerian wavenumber spectrum, $E(k) = \alpha_1 \varepsilon^{2/3} k^{-5/3}$, as $\alpha_1 = \frac{1}{3}(4\pi)^{2/3} \simeq 1.802$, and in the Lagrangian frequency spectrum, $E(\omega) = \beta_1 \varepsilon \omega^{-2}$, as $\beta_1 = 2$. The unique values for α_1, β_1 and κ are situated well within the broad scatter range of observational, experimental and approximative results. Our derivations rest on geometry, methods from many-particle physics, and on elementary conservation laws.

1. Introduction

In the present paper we show that fluid turbulence can be understood in an idealised sense as a statistical many-body ensemble – a tangle of vortex tubes taken as *discrete* particles. We follow an early conjecture by Ludwig Prandtl [1926] who discussed an analogy between molecular diffusion and turbulence. He

related his mixing length¹ or *Mischungsweg* with the mean-free path of kinetic gas theory and considered his fluid elements or fluid lumps (*Flüssigkeitsballen*) of locally nearly same size as relatives of gas molecules. He further assumed his mixing length to scale with the “di-

¹According to Hinze [1953] also G. I. Taylor made early use of the notion *mixing length*.

ameter” of his fluid elements.

Although purely heuristic, his concept became popular in the years before WW2. The question how to compute the details could not be answered without reference to measurements. After WW2 the gas-kinetic analogy found thus strong criticism from the continuous-image side [see Introduction in Batchelor, 1953]. This was plausible because the gas analogy represents a *discrete* concept that, if useful, would label a Copernicanian turn or a paradigm shift in our grown view of turbulence as an exclusive matter of *continuum* mechanics.

In this situation Werner Albring [1981], in the footsteps of Prandtl, explicitly challenged the continuous paradigm of Reynolds [1895], Keller and Friedmann [1924], Taylor [1935], Batchelor [1953] and their many followers, when he posed the fundamental question:

Can the Navier-Stokes equation be used to calculate turbulent flows?

His doubts were based on the feeling that the continuous image of RANS does possibly override features of most elementary vortex interactions at small scales.

In analogy to Albring one might ask: Can we deduce a rose’s blossom from the periodic system of chemical elements? Intuitively we answer with *no*. However, this answer is justified because generally “more is different” [Anderson, 1972].

Looking in this sense at Albring’s above question we may add that the prediction horizon of the Navier-Stokes equation (NSE) is strongly limited by a series of higher-order non-equilibrium phase transitions when a growing Reynolds number goes through a number of critical values. In these super-critical regions the sensitivity against initial conditions becomes relevant and leads to the famous butterfly effect [Lorenz, 1963]. This is closely related with irreversibility. At least in the limit of vanishing viscosity the initial-value problem for NSE looks like a *reversible* one. But we know that turbulence at $Re = \infty$ is an *irreversible* process.

In principle this problem was already known by Poincare and others as an aspect of the three-body problem of celestial mechanics, but in a fluid-mechanical context it has been demonstrated only after WW2 by Lorenz [1960, 1963]. Without going into details of the onset of turbulence and non-equilibrium phase transitions in hydrodynamics and their reflections in various branches of pure mathematics, together with Prandtl and Albring we hypothesize that NSE is *not* sufficient to understand the secrets of turbulence or to even predict turbulent flows, in particular not in the

limit $Re \rightarrow \infty$. Some readers might even go a step further and argue that higher-order elements of the Friedman-Keller expansions of NSE, e.g. the second and third-order turbulence closures discussed in Voropayeva [2007] and the literature quoted therein, as well as the various “corrections” of those closures populating turbulence theory, are modern analogues of the epicycles of geocentric times. But this would exceed the limits of the present report. In this respect we better refer to the agreeable picture of today’s status of turbulence science drawn by Davidson [2004] in the preface of his book where he mentions even “religious wars. . . between the different camps” of turbulence theory.

There are not many physical phenomena resisting theoreticians so long like turbulence. In the past it was mainly supra-conductivity which took about 30 years [Feynman, 1963]. Today similarly obstinate problems are dark matter, dark energy, and super-symmetry which have also now an age of about up to 40 years. But turbulence waits still much longer for redemption and remained particularly as *the* very last unsolved enigma of *classical* physics.

Below we develop an asymptotically invariant alternative to RANS and higher-order closures, which is not primarily based on NSE but does not violate NSE either.

Although the theory of many-particle physics offers a huge reservoir of potentially helpful methods and tools, a closer inspection reveals that the number of *directly* applicable tools is less impressive. Neither Liouville theorem, ergodic hypothesis or Hamilton formalism nor other concepts for thermodynamic equilibrium are applicable in their classical forms. Turbulence is essentially an open-system, thermodynamically non-equilibrium phenomenon. In best cases we have a steady state or *Fließgleichgewicht* in the sense of Bertalanffy [1953], Glansdorff and Prigogine [1971] and Haken [1978, 1983]. However, the concepts of Ising about particle dressing, quasi-particles and renormalization – in the broader sense of Dresden [1993] and McComb [2004] – appeared as essential guidelines in the slow evolution of our thoughts.

Surely, turbulence can successfully be attacked from more than one side². Whereas the continuous image has led to a number of important results, for instance RANS and the broad spectrum of different heuristic closure

²Theories generally compromise portrait and design aspects and in some case mathematically different images of turbulence will show up eventually as fully equivalent in their physical predictions, like Heisenberg’s matrix mechanics and Schrödinger’s wave mechanics.

schemes discussed e.g. by Wilcox [2006], without additional phenomenological input it gave neither unique values of the universal constants of turbulent motion like von-Karman’s and Kolmogorov’s spectral constants nor a *closed* image of turbulent flows. This has led to the following view shared by many theoreticians [Landaу and Lifshitz, 1987, p. 173]:

... and κ (is) a numerical constant, the *von Karman constant*, whose value cannot be calculated theoretically and must be determined experimentally. It is found to be $\kappa = 0.4$.

In this respect one can actually be more optimistic. Frictionless turbulence is governed in a weak sense by the Euler equation, a special case of NSE. The Euler equation together with the conservation of mass represent pure “inert geometry”. We can thus expect that the universal constants of turbulent motion are ruled by certain geometrical constants, e.g. by irrational numbers like $\sqrt{2}$ and/or transcendental numbers like π . Indeed, this is possible. In a precursor study based on the particle picture used also below, von Karman’s constant could be derived as $\kappa = 1/\sqrt{2\pi} \simeq 0.399$ [Baumert, 2009]. This interesting result led to the conjecture that the particle concept can give also insight into spectral aspects of turbulence.

Below we make explicit use of theoretico-physical thinking, which differs from other scientific activities like computer modelling and mathematical physics, from applied mathematics, and from the measuring and observational disciplines.

Computer modelling and measurements have in common that they deal with really existing, *finite* systems and data, in particular with *real* and *integer* numbers, with variables of *finite* size.

Theoretical physics, however, deals with “things” which never did, which do not and never will exist: e.g. with point masses, homogeneous continua, idealized vortex tubes, linear waves, frictionless fluids, plane and impenetrable walls, infinitely small or large variables. A further building block of theoretical physics is an often unspoken principle which we apply also here: it “dictates that, all things being equal, one goes for the simplest possibility—a rule that has worked remarkably well.” [Zee, 1986, p. 85, see also Chandrasekhar, 1979]. Sometimes this principle is called Occam’s razor.

Mathematics also deals with similar non-existing objects, but their relations to the real world are outside its responsibility. It is the responsibility of theoretical physics to relate idealized thought systems with the real

world. The following report concentrates solely on the latter aspects.

With one exception, the following text contains no “fancy shmancy mathematics”. It is the relation between equations (7), (8) and (9) that would need some time to be derived from scratch. Fortunately, this has already been done by other authors many years ago and went into the textbooks on stochastic-dynamic systems [e.g. Kraichnan, 1968; Haken, 1978, 1983; Stratonovich, 1992, 1994] to which we refer the theoretically interested reader. We further suggest to begin first with Baumert [2009] because it is actually the basis of the present report.

Everywhere the pronomen “we” is used in this text, it means the two of us, the dear reader and the author.

2. Particles

If we take Prandtl’s discrete particle concept seriously but not literally, then a number of questions need to be posed – and answered. A first question to be addressed is the following.

Where do the particles come from? With respect to their substance our particles are indistinguishable from their fluid or gaseous environment. It is only their state of motion which makes the difference to the surrounding fluid so that we better should talk about quasi-particles, but keep for brevity the term *particles* in the following. They are characterized by their geometry, their specific kinetic energy, by their vectors of linear and angular momentum.

Our particles are generated as representatives of turbulent fluctuations such that their energy has to be drawn from the mean flow field via so-called shear production³ to keep the total kinetic energy of the flow in balance. I.e. if there is a shear in the mean flow and non-vanishing turbulent viscosity, then the mean flow *looses* kinetic energy which reappears in form of TKE⁴, i.e. as energy of vortex motions. Hereby an exact process description of vortex *generation* is not needed as long as we know *how much energy* is lost and *how much vorticity* is generated so that we can place vortices of corresponding properties into the flow. In a way we may talk about an *emergence* of the particles.

³Convective turbulence and internal-wave breaking will be treated in another study.

⁴In the following the word turbulent kinetic energy or TKE is often used. In the given context it means actually a kinetic energy *density*, i.e. energy per unit of mass. Therefore we measure TKE most comfortably in the units $\text{m}^2 \text{s}^{-2}$.

What do the particles look like? Due to Helmholtz’ principle of conservation of circulation, a circulation-free fluid volume should exhibit zero circulation over the course of time. I.e. particle generation cannot add any circulation to the volume. This implies that turbulence production can take place only in form of the generation of *couples* of counter-rotating vortices with zero total circulation. Consequently we specify Prandtl’s fluid elements as *dipoles* where the simplest form is locally fully symmetric, which is to be understood in a statistical sense.

This assumption is central for our theory but deserves a comment. It is well-known that in laminar and turbulent flows wall friction generates velocity gradients or current shear, which is identical with circulation induction into the mean flow. This process is governed by RANS, more specifically by its turbulent friction term containing correlators like $\langle u' w' \rangle$, i.e. by the Reynolds tensor. This tensor is calculated further below on the basis of a particle theory. If a particle would have own circulation on the local level, it would add extra circulation to the flow, which would violate RANS. Our particles can therefore have no own circulation.

Thus we have the challenging theory situation that a mean flow exhibits turbulent friction and circulation while the turbulent vortices responsible for fluctuations and friction have no circulation and are essentially frictionless, excepting the singular dissipation scale of size zero, see further below.

With respect to the specific form of vortices in our dipoles we refer to the classical notion of *vortex tubes* wherein vorticity is confined to the interior of a tube of smaller or larger cross section [see further below and Pullin and Saffman, 1998, who quote papers by Kuo & Corrsin, 1972, and Brown & Roshko, 1974, showing tubes as dominating characteristic structures]. A nice and more recent study of vortex tubes has been presented by Wilczek [2011] who also published on the internet a number of valuable animations of vortex ensembles in motion⁵. We note that, as always, the centerlines of our vortex tubes form either closed loops or they are attached to boundaries.

Ordinary linear momentum of a dipole is known from classical theory in local approximation and can be imagined in analogy to the motions of smoke rings. It is conserved in our many-particle image if each particle, generated in a locally homogeneous volume element, exhibits no preferred direction of motion. The linear mo-

mentums of two dipoles with opposite directions compensate each other. Assuming a locally “sufficiently high” and *even* number of dipoles thus guarantees that the particle-induced linear momentum and circulation are zero and total momentum of the flow exclusively governed by the mean-flow momentum balance including the Reynolds stress terms.

How do the particles move? The motion of a single isolated dipole [a “naked” particle in the terminology of many-particle physics, see e.g. Dresden, 1993; McComb, 2004] can be given by classical rules [see Lamb, 1932; Albring, 1981; Saffman, 1992; Baumert, 2005b, 2009]. However, if the selected dipole is embedded in a dense tangle and thus surrounded by a cloud of similar dipoles, its properties are “screened” by the cloud and thus modified: it appears to be “dressed” – without violation of governing conservation laws. The solution is discussed in the next section.

3. Vortices, energy, and scales

Traditional vortex models

The hydrodynamic literature presents a larger number of elementary analytic models for single isolated vortices under different conditions. Whereas the so-called potential vortex is less realistic, the Oseen vortex, the Rankine and the Taylor vortex, the Burgers, the Lundgren, and the Long, the Sullivan and the spherical Hill vortex are more realistic models of isolated vortices far from others and from boundaries [for overviews see Lamb, 1932; Lugt, 1979; Albring, 1981; Saffman, 1992; Pullin and Saffman, 1998; Davidson, 2004].

Excepting the potential vortex, all other vortex models are principally realistic and show first a core with radially increasing tangential velocity, then a saddle, and then a tail wherein the tangential velocity decreases radially down to zero. However, in our context these models are not applicable because they hold for conditions of isolation only. They cannot be transferred to conditions of a dense vortex tangle where the distance between vortex dipoles is small and the surrounding cloud of similar vortices screens the effects from the rest. Therefore a new approach is needed, without violating governing conservation laws, neither on a global nor on the scale of the locally homogeneous and isotropic fluid volume.

I.e. an ideally “dressed” vortex dipole moving frictionless within a tangle of similar objects should necessarily be characterized by a finite *effective* radius, r , within which all the kinetic energy, \mathcal{K} , and vorticity of the vortex is concentrated so that we may talk of an “energy-containing radius”. For simplicity, in a statisti-

⁵<http://pauli.uni-muenster.de/tp/menu/forschen/ag-friedrich/mitarbeiter/wilczek-michael.html>

cal sense r and ω are taken identical for the two vortices forming the internally symmetric dipole.

We summarize as follows:

- The effective scales ω and r are governed by local conservation of energy and angular momentum.
- The radius r defines a boundary within which kinetic energy and vorticity of a vortex are confined.
- The effective tangential velocity of a vortex is $u = \omega r$ and equals the propagation velocity of the dipole. The resulting kinetic energy of the dipole is thus $\mathcal{K} = 2 \times u^2/2 = 2 \times r^2 \omega^2/2 = (r\omega)^2$.
- The vortices are incompressible but deformable quasi-solid bodies which move frictionless in the vortex tangle. I.e. vorticity is uniformly distributed within the cross-section of a vortex tube and has the value $2 \times \omega$.
- At solid boundaries vortices perform frictionless roll motions. Dissipation happens exclusively *within* the fluid at scale zero. (In reality the dissipation interacts with boundaries through heat and sound generation.

These assumptions describe our image of vortices in a turbulent vortex tangle without violating the conservation laws of kinetic energy, momentum, angular momentum and circulation. Compared with the above-mentioned vortex models our approach may be interpreted as a renormalization procedure leading to a finite kinetic energy and a finite spatial extension.

While on a first glance this procedure looks somewhat arbitrary, exactly this image is well established since long in physical oceanography, which is a world of highest Reynolds numbers. In physical oceanography, meteorology and physical limnology the a.m. characteristic radius, r , is traditionally related with the “energy-containing” scale, which is a direct observable under conditions of stable stratification and related with the so-called overturning and Thorpe scales. Central aspects are discussed in detail in the following section.

Vortex tubes and rigid-body rotation

In stable stratification turbulent vortices are directly recognizable in vertical profiles of density, ρ , and other scalar variables, such as temperature and salinity, as “overturning” of density profiles. Within certain energetic limits they move heavier over lighter fluid and thus produce a direct imprint of the vortices in instantaneous depth profiles of density, $\rho(z)$. This imprint

has a *unique* character in stratified flows because the buoyancy force implies that there should be a stably stratified “reference” state, $\bar{\rho}$, a state in the absence of turbulent overturning.

This imprint appears typically as a Z-pattern, see Fig. 1, which obviously stands for a solid-body rotation wherein the tangential (azimuthal) velocity grows linearly with the radius coordinate up to a maximum at its outer radius and then (outside the body) drops rapidly down to zero. We interpret a Z-pattern as a realisation of a vortex embedded in a dense vortex ensemble. i.e. as a so-called *rigid vortex* as discussed by Lugt [1979] and further below⁶.

To our knowledge, the use of overturning deviations from the stable state to derive vortex radii was first introduced and explored by Thorpe [1977] in an analysis of temperature profiles from Loch Ness, Scotland. Thorpe showed how the reference state can be reconstructed from measurements and how overturns and overturning scales can be detected. His approach is a solid basis to measure the radii (or diameters) of vortices in stably stratified fluids directly.

Thorpe [1977] described the general case of a *monotonous* reference density distribution and the overturning fluid body as *frozen* for the time of the overturn. This is justified as long as the length achieved through molecular diffusion during the time of rotation, $l_d = \sqrt{2\nu_m t_{ot}}$, is *small* compared with the energy-containing radius r of the overturn⁷. In water this condition is always satisfied as l_d remains here in the range of centimeters and less.

Later authors like Imberger and Boashash [1986] considered a subset of the monotonous case, the *linear* reference-density distribution as depicted in our Fig. 1. Itsweire et al. [1986] in their Fig. 1 were the first to describe the overturning motion explicitly as the effect of a rigid-vortex motion [cf. also Pullin and Saffman, 1998].

Thorpe’s method in oceanography

Background. A short digression on the background of Thorpe’s method might be in place. Geophysical fluid dynamics is a domain of pioneering turbulence stud-

⁶ The idea of a rigid vortex is compatible with fluid mechanics because Helmholtz’ laws also apply here. But the connection with continuum mechanics is not trivial because the velocity distribution in a rigid vortex exhibits a singularity at the outer radius where it drops from a finite value down to zero. Further, the isolated rigid vortex is not stable.

⁷ Here ν_m is molecular viscosity and t_{ot} the duration of an overturn at the energy-containing scale $r \propto L$.

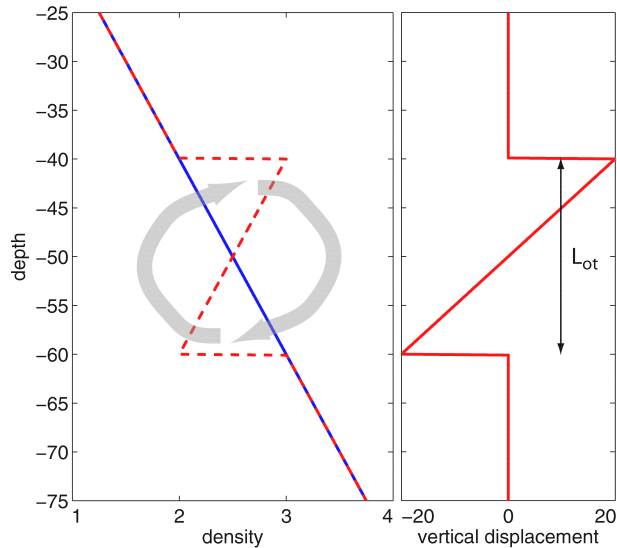


Figure 1. Overturning and overturning scales in the sense of [Imberger and Boashash, 1986, Fig. 6 there]. The cartoon depicts a 180° overturning of a 20 m thick layer that brings relatively heavy water up and lighter water down. Note the characteristic Z-pattern of the vertical displacement ζ . The original stable density profile is the blue line, the unstable density in the overturn is red and dashed. By courtesy of Dr. Hartmut Peters, Earth and Space Research, Seattle, USA.

ies at high Reynolds numbers because atmosphere and oceans offer the necessary conditions for free. The first massive demonstration of measured Kolmogorov spectra was carried out by Grant et al. [1959] at a Reynolds number of about $Re \approx 10^8$ in a 100 m deep tidal channel⁸. They demonstrated the validity of the 5/3 law over an interval of 3.5 orders of magnitude (about 12 octaves). Together with the logarithmic law of the wall and the decay of TKE in homogeneous isotropic turbulence according to t^{-1} [or $(x/U)^{-1}$ in the wind tunnel; cf. Batchelor, 1953, Chapter VII] the 5/3 law belongs until now to the most prominent universal features of high- Re turbulence.

Many observational techniques and dynamical concepts of geophysical fluid dynamics were first developed in meteorology and later adopted in physical oceanography and limnology. That this was not the case with turbulent overturning is likely related to the fact that the troposphere, the most accessible part of the atmo-

sphere, does not show consistent mean stratification. In contrast, oceans and lakes are almost everywhere stably stratified outside of boundary layers. It further makes sense that turbulent overturning was first explored in a lake where temperature, T , is the sole stratifying agent. In contrast, ocean stratification depends on temperature as well as salinity, S , and density $\rho = \rho(p, T, S)$ cannot be measured with the same resolution as T alone. We note in passing that real fluids are compressible such that analyzes of overturning scales have to be based on potential density and potential temperature.

The imprint of turbulence in vertical density profiles allows defining and extracting overturning scales such as the Thorpe scale, L_{Th} [Thorpe, 1977]. The cartoon of Fig. 1 illustrates the overturning of a $L_{ot} = 20$ m thick layer of the water column by a single vortex in solid body rotation of diameter L_{ot} . According to our above discussion of vortex dipoles as quasi-particles we conclude that $L_{ot} = 2r$.

The graph depicts the moment after a 180° rotation that brings heavy water up by vertical displacements with a range of $\zeta = 0 \dots +L_{ot}$ and moves lighter water down by $\zeta = 0 \dots -L_{ot}$. The Thorpe scale is defined as the r.m.s. of ζ . The linear original density profile of the cartoon implies

$$L_{Th} = L_{ot}/\sqrt{3} = \frac{2}{\sqrt{3}} r = 1.15 r. \quad (1)$$

We define ζ by the path from its original depth to a displaced depth. That is, ζ carries the same sign as the vertical turbulent velocity w' that has caused it.

Fig. 1 may seem simplistic. It can easily be made more realistic by adding that, in the course of the overturning, and owing to the unstable stratification within overturns, flow instability will occur and generate turbulence and a range of smaller scales than L_{ot} , inside the big overturn.

The ocean is full of overturns that look just like this scenario. Fig. 2 depicts a big overturn in the Pacific Equatorial Undercurrent, EUC, on the equator at $140^\circ W$ from Peters et al. [1995]. Note the Z-shape of the big overturn and its sharp upper and lower edges.

In oceanography and limnology, Thorpe's concept of vortices overturning parts of the water column are applied to observations as in Fig. 2. Measured potential density (σ_Θ ; by convention 1000 kg m^{-3} is subtracted) or potential temperature (Θ) data points are "Thorpe-sorted" into monotonically rising or falling sequences corresponding to stable density stratification. The sorted profiles are taken as a proxy for the refer-

⁸Today's DNS of turbulent flows do not exceed $Re \approx 10^5$ and even the European superpipe CiCLOPE will in the best case not significantly exceed $Re \approx 10^6$ [Rüedi et al., 2009].

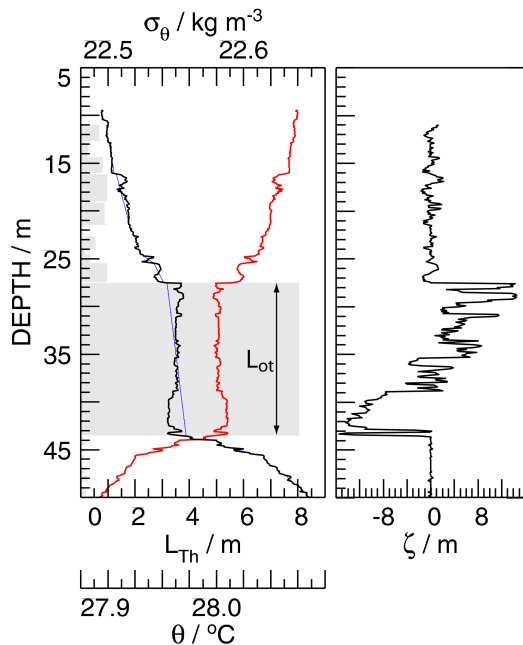


Figure 2. A big overturn in the Pacific Equatorial Undercurrent at 0°, 140°W during the Tropic Heat II cruise [Peters et al., 1995, adapted from]: (a) potential temperature (Θ , red) and potential density (σ_Θ , black), Thorpe-sorted σ_Θ (blue), and Thorpe scale L_{Th} (shaded); (b) turbulent vertical displacement ζ . By courtesy of Dr. Hartmut Peters.

ence, or “mean” profile that gave rise to the observed turbulence and overturning. The vertical distance over which data points have to be moved to make the profile monotonic is $-\zeta$. I.e. Thorpe-sorting “undoes” the overturning. Individual overturns are defined by $\sum_i \zeta_i = 0$ [Dillon, 1982].

The shaded bars in Fig. 2(a) show L_{Th} averaged over individual overturns. This definition is highly robust. A squared buoyancy frequency N^2 computed from the sorted σ_Θ or Θ is non-negative⁹, $N^2 \geq 0$.

Turbulent length scales related to overturning scales are unaffected by the presence of internal gravity waves (IGWs). IGWs are ubiquitous in stratified geophysical flows and dominate velocity and scalar spectra at vertical scales of the order of $O(100 \text{ m})$ and smaller [e.g. Peters et al., 1995]. The TKE accounts only for a tiny fraction of the integral of these “red” spectra. Owing to this property, length scales commonly used in lab-

⁹ Here we may restrict our considerations to incompressible fluids where $N^2 = -g/\langle\rho\rangle d\langle\rho\rangle/dz$ with g as gravitational acceleration, $g = 9,81 \text{ m s}^{-2}$.

oratory experiments, such as the Ellison [1957] scale, $L_E = \overline{\rho'}/\langle\partial\langle\rho\rangle/\partial z\rangle$, are unsuitable for a characterization of turbulent length scales in geophysical flows because density fluctuations $\rho' = \rho - \langle\rho\rangle$ inevitably are dominated by IGW signals so that L_E can no longer be interpreted as a characteristic length scale of turbulent fluctuations. Here, angular brackets denote ensemble averages $\overline{\rho'} = \langle\rho'^2\rangle^{1/2}$ is an r.m.s. value.

Thorpe scale and Taylor scaling. The great power of Thorpe’s [1977] concept can be demonstrated by considering the so-called Taylor scaling, with q as an r.m.s. measure of turbulent velocity fluctuations. Dimensional analysis strictly gives for l as an energy-related length scale the following:

$$l \propto q^3/\varepsilon. \quad (2)$$

Here l is obviously related with TKE because of $\overline{\mathcal{K}} \propto q^2$, and ε is the TKE dissipation rate¹⁰.

If the Thorpe scale *is* indeed a measure of the size of the energy-containing vortices and thus related with the energy-containing scale, i.e. $L_{Th} \propto l$, then we can write (2) as follows,

$$\varepsilon \times L_{Th} \propto q^3, \quad (3)$$

or

$$q \propto (\varepsilon \times L_{Th})^{1/3}. \quad (4)$$

Instead of q one can alternatively use $\overline{\mathcal{K}}^{1/2}$ with turbulent kinetic or mean vortex kinetic energy, $\overline{\mathcal{K}}$. Fig. 3 shows measurements in the ocean demonstrating that relation (4) is true, in a statistical sense. The Thorpe scale characterizes indeed the size of the energy-containing eddies.

However, this statement needs a comment. Thorpe-sorting as a technique to measure the radius or diameter of energy-containing turbulent vortices rests on the existence, and hence works only, in stratified flows. Under geophysical conditions this automatically implies that a certain coexistence of IGWs and turbulence is inescapable. The q in (2) must only reflect TKE and must not be contaminated by the much larger IGW energy.

While the separation of waves and turbulence is beyond the scope of this note¹¹, a workaround is to consider spectra and to study only the ultra-violet

¹⁰We use the convention that the symbol \mathcal{K} denotes the energy of one selected dipole whereas $\overline{\mathcal{K}}$ is the local average of the same variable for a whole ensemble

¹¹The reader is referred to Peters et al. [1995] and D’Asaro and Lien [2000].

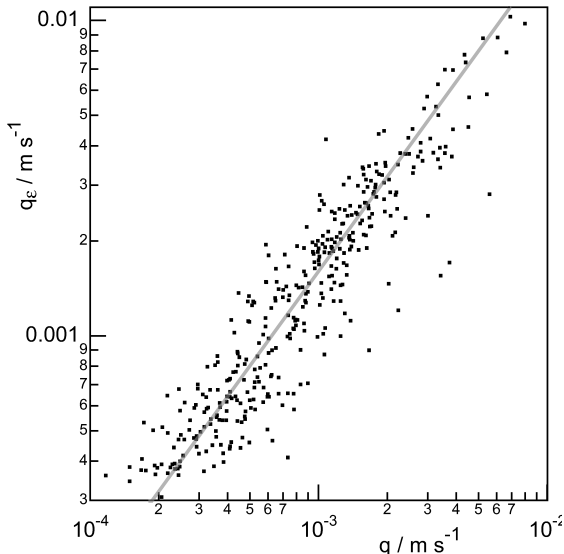


Figure 3. Turbulent velocity $q_\epsilon = (\epsilon l)^{1/3}$ derived from measured ϵ via Taylor scaling, (4), versus measured turbulent velocity fluctuation q . Adapted from Peters et al. [1995] where $l = 1.6 L_{th}$ and where q is the spectral velocity variance at vertical wavenumbers $\geq 1/l$. Shown are data for individual overturns at least 1 m thick from depths 60–350 m in the Equatorial Undercurrent at 0° , 140°W . The gray line indicates the median ratio of q_ϵ over q . By courtesy of Dr. Hartmut Peters.

or short-wavelengths part where IGW existence is excluded through their dispersion relation. Peters et al. [1995] did exactly this and extracted q from oceanic observations as the velocity variance at scales of l and smaller. On this basis, Taylor scaling clearly emerges from their observations (Fig. 3).

Thorpe’s [1977] concept of turbulent vortices and their imprint through vertical overturning on density profiles allows extracting energy-scale variables even in conditions where velocity and scalar spectra are heavily dominated by internal gravity waves. It allows relating energy-scale- to dissipation scale variables through the turbulent length scale that carries Thorpe’s name. These *directly observable* energy-containing length scales stand for the radius or diameter of our renormalized vortices discussed further above.

Dressing a rigid-vortex tube

As we learned from the considerations and examples above, turbulence may be imagined as vortex tubes resembling a dense “local cloud” of dipoles in chaotic mo-

tion, the cloud having zero angular and linear momentum. So far the rigid-vortex tubes have been considered as somewhat arbitrary idealizations of real-world vortices.

Translated into the language of home cooking, a snapshot of rigid-vortex turbulence may be imagined as a dense, entangled heap of hot spaghetti arrabiata. The spaghetti rotate around their inner centerlines and move frictionless within the (inviscid) sauce arrabiata. Therefore the only interactions between individual spaghetti occurs when they touch each other randomly.

It arises the question whether the rigid-vortex tube and a corresponding dipole is a *stable* solution of the Euler equations. We leave it to the interested reader to derive from these equations that an isolated rigid vortex indeed solves these equations, but, as long as it exists, generates the following pressure head as a consequence of inertial (centrifugal) forces:

$$p = p_0 + \frac{\rho}{2} \times \omega^2 r^2. \quad (5)$$

Here p_0 is the background pressure of a laminar reference flow, e.g. in the ocean the depth-depending hydrostatic pressure. If the pressure outside the vortex would simply be p_0 then, due to the action of the outwards-directed pressure head of the vortex motion given by the second term in (5), the vortex would loose stability.

The stability of quasi-rigid vortices as observed in real-world turbulence can thus be guaranteed only by the help of a compensating force of equal strength. Here a concept of many-particle physics comes into play: dressing. As far as we will embed our initially isolated rigid vortex into a locally homogeneous and isotropic large ensemble (“cloud”) of *similar* vortices (more precisely: dipoles made of rigid vortices), the members of the cloud generate more or less exactly the counter pressure needed to compensate (5) and keep the vortex “stable enough”.

According to (5) and with $u = \omega r$ the pressure deviation can be written as follows,

$$\delta p = p - p_0 = \frac{\rho}{2} \times u^2 = \rho \times \mathcal{K}, \quad (6)$$

where \mathcal{K} is the kinetic energy density in a vortex. Obviously the measurement of turbulent pressure fluctuations can help estimating turbulent kinetic energy. This corresponds to an early classical but approximate result of continuum theory [eq. (8.3.21) on p. 182 in Batchelor, 1953; Hinze, 1953, p. 242, last eq.]. We will not explore the potential of (6) further and leave it to the interested reader.

4. Turbulence and kinetic gas theory

Similarities

About 150 years ago, James Clerk Maxwell presented his kinetic theory of gases. Even if the details of molecular interaction forces in vacuum would have been known that time, it would have not been helpful. An integration of Newtons law of motion in terms of ordinary differential equations for each one of the billion particles was practically excluded. But the creative use of symmetries and conservation laws radically simplified the situation and led eventually to a closed description of the most important macroscopic properties of gases. Main elements are the following:

- (i) The particles in a gas are perfectly elastic *points* with non-zero mass.
- (ii) They are in permanent random motion which is to be described in terms of statistical moments and sometimes called “molecular chaos”. The scatter motions exhibit no preferred directions.
- (iii) The collision results depend only on the local angular orientation of the collision partners.
- (iv) Between collisions they move uniformly and independently, without preferred direction.
- (v) Due to chemical neutrality, collisions lead only to the scatter of trajectories.

The corresponding “turbulent relatives” of the above are:

- (i') The particles are locally symmetric vortex-dipole *tubes* with finite cross-sectional area, with vorticity and kinetic energy confined in the tubes, and with zero circulation.
- (ii') Their random translatory motions prefer no directions and may be termed ‘dipol chaos’ [Marmanis, 1998].
- (iii') The result of collisions depends only on the local angular orientation of the colliding dipole elements.
- (iv') Between collisions the particles move along complex trajectories which may be curved.
- (v') For symmetry reasons, 50 % of all collisions occur between two *counter-rotating* dipole elements leading to dipole recombinations [or reconnections, like those reported in a turbulent superfluid by Paoletti et al., 2010] and at the end to

quasi-elastic, random scatter motions resembling turbulent diffusion and mixing, see left branch in Figure 4.

We underline that these rules shall apply only locally in space and time. Of course, the prediction of the global pathway of a vortex dipole is impossible.

Differences

Major differences between ideal gases and turbulence are the following:

- (a) The number of chemically neutral gas particles in a container is constant in time. They form a closed thermodynamic system. There is no particle annihilation.
- (b) The particles of turbulence are excited energy states, their number decreases via collisions and subsequent energy dissipation. They need to be replaced by shear generation of new particles if their number shall be kept more or less in balance.
- (c) In a gas, trajectories of point masses are simple *lines* in space, trajectories of vortex-dipole tubes produce curved *areas*.

While gases evolve towards static thermodynamic equilibria, turbulence evolves either towards *dynamic* equilibria or steady states¹², which may have periodic character, or turbulence dies off.

To specify this important difference we have to supplement our above property list for “turbulence particles” as follows:

- (d) For the same symmetry reasons like in (v') of section 4 above, the remaining 50 % of all dipole collisions occur between two *likewise rotating* dipole elements. Each case generates a fundamentally unstable vortex couple forming a slowly rotating dissipative patch with its center of mass more or less at rest. This patch decays through turbulent dissipation in the special form of a “devil’s gear” or Kolmogorov spectrum. For details see further below and the right branch in Fig. 4.

¹²This neither implies homogeneity, equifinality nor uniqueness of steady states.

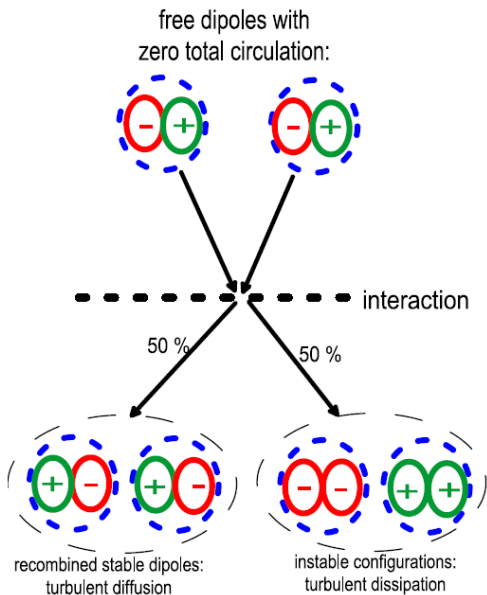


Figure 4. Two possible collision results of two dipoles: the left branch is “diffusive” because it leads to a recombination of the dipole elements and scatter of trajectories which is known as turbulent diffusion. The right branch is “dissipative” because it leads to an unstable vortex configuration which decays “somehow” into heat¹⁴. For symmetry reasons both branches have identical probabilities of 0.5. Note that the circular form of the vortex cross sections presented here are chosen for reasons of clarity. They hold as an statistical average picture only. Real vortices have elliptic or even strongly deformed cross sections.

5. Equations of turbulent motion

Brownian and turbulent motions

The turbulence properties (iii’) and (v’) of section 4 above establish an analogy of turbulent dipole movements with the Brownian motion of particles suspended in a fluid at rest [in the sense of Einstein, 1905]. In the present turbulent case it is not the kinetic theory of heat which governs the motions, it rather is Helmholtz’ theory of dipole motions.

The (local) temporal path increments $\delta\vec{Y}_j$ of a vortex dipole j may be found by integration of the following Langevin equation over the time increment δt ,

$$\frac{d\vec{Y}_j}{dt} = \vec{V}_j, \quad j = 1 \dots \mathcal{N}, \quad (7)$$

where \vec{V}_j is the random center-of-mass velocity of the selected dipole j .

To specify the stochastic process $\vec{V}_j = \vec{V}_j(t)$ as simple as possible, we choose a zero-mean, white-noise Gaussian process. Its strength is controlled by the locally averaged dipole properties $\bar{\mathcal{K}}$ and $\bar{\omega}$. More elaborate random processes like the Ornstein-Uhlenbeck or the Kraichnan model [Kraichnan, 1968] and others are beyond the focus of the present paper.

We now need to make a bigger jump over the broad river of stochastic dynamic systems theory where the probability density function for the solution of a dynamic system¹⁵ may easily be taken from applied textbooks like those of Haken [1978, 1983] in form of solutions of the Fokker-Planck equation (FPE) corresponding to the extremely simple stochastic-dynamic system (7). In the present case the FPE reads as follows,

$$\frac{\partial \mathcal{N}}{\partial t} - \frac{\partial}{\partial \vec{x}} \left(\nu \frac{\partial \mathcal{N}}{\partial \vec{x}} \right) = 0, \quad (8)$$

where \mathcal{N} is the probability density mentioned above, an equivalent of the particle number density itself. ν characterizes the strength or intensity of the noise $V_j(t)$ in (7). As already mentioned it is governed by the control variables $(\bar{\mathcal{K}}, \bar{\omega})$ and appears later as coefficient of eddy diffusivity of momentum, i.e. as eddy viscosity.

In the transition from (7) to (8) it has implicitly provided that all gradients exhibit sufficiently smooth and slow behavior. Those local quasi-equilibrium conditions are typically assumed in non-equilibrium thermodynamics and many-particle physics. This clearly excludes shocks and steep fronts from our considerations.

A further comment concerns an assumption used implicitly above. It is an analogue of the so-called Ising assumption known from the theory of magnetism: we treat triple or higher interactions between vortex filaments as negligible¹⁶.

¹⁵A dynamic system is here understood as a set of possibly non-linear ordinary differential equations driven at their right-hand sides by stochastic processes.

¹⁶This is not fully trivial. Under specific conditions of Bose-Einstein condensates stable configurations consisting of one vortex and two anti-vortices have been observed in the laboratory, either in linear setups or equilateral triangles [Seman et al., 2009]. The latter is most symmetric and called a *tripole*. Here we assume that in our very dense “vortex gas” tripole-tripole interactions are controlled by dipole-dipole interactions of their subsets. Note that tripoles might violate the principle of zero circulation on the level of elementary interactions needed to keep the mean-flow momentum balance in correct balance.

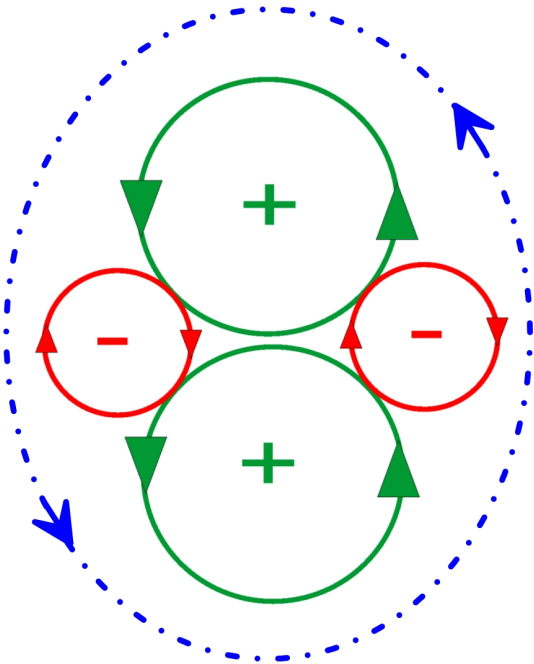


Figure 5. Local cross section through the first developmental stage of an unstable pair of likewise rotating vortices resulting from a dipole-dipole collision (right branch in Fig. 4). The green circles represent the primary energy-containing vortices with identical radii r . Note that the green circles do *not* touch each other! They are separated by the red circles who symbolize secondary vortices in the beginning phase of a whole vortex cascade. The dipole cloud surrounding the above structure not only generates the necessary pressure head to keep individual vortices stable but it also acts as a source of perturbations initiating roll-up instabilities and thus tertiary and higher-order vortices and eventually a fully developed dissipative patch, see text. The broken blue line and the arrows symbolize the slow rotation of the whole patch around the common center of mass.

Generation and annihilation of particles

Property (d) in Section 4 above allows to supplement the right-hand side of equation (8) with sink and source terms, leading to a reaction-diffusion type equation:

$$\frac{\partial \mathcal{N}}{\partial t} - \frac{\partial}{\partial \vec{x}} \left(\nu \frac{\partial \mathcal{N}}{\partial \vec{x}} \right) = \Pi - \beta \mathcal{N}^2. \quad (9)$$

Here Π is the rate of quasi-particle generation. It is to be expressed in terms of kinetic energy per unit time and is thus necessarily proportional to the energy loss of the mean flow.

The second term corresponds to the energy-dissipation rate of TKE, ε , i.e. TKE conversion into heat and/or sound, with β being a constant [for details see Baumert, 2009]. ε scales with the rate of particle annihilation resulting from collisions. As we learn from chemical kinetics [see Haken, 1978, 1983, for details], the annihilation term is quadratic in the particle number, \mathcal{N} , because *two* particles need to collide to generate *one* unstable couple which is then converted into heat and/or sound. This is discussed in the next Section.

6. Dissipative patches

Formation of vortex spectra

Our Fig. 4 and the concept behind it may seem simplistic. It demonstrates the only two possible results of a dipole collision. While the left half of the Figure shows the recombination of *counter*-rotating vortices from counter-rotating vortices, the right half shows the formation of a couple of *likewise* rotating vortices from counter-rotating vortices. If isolated or naked, the likewise rotating couple revolves around a common center of mass and remains thus nearly at rest. This couple is known to be unstable, to form stationary dissipative patches [Sommerfeld, 1948]¹⁷.

This picture with the dissipative patch almost at rest implies that dissipation is a spatially patchy phenomenon called *intermittency* and studied extensively by various authors [for an overview see e.g. Frisch, 1995]. We do not go into details because intermittency is outside the focus of this study. We discuss instead the way *how* the unstable configurations at the right half of Fig. 4 and in Fig. 5 could be transformed into a Kolmogorov-Richardson spectrum. This problem has attracted early attention by Taylor [1937] and Kolmogorov [1941]. The latter found on dimensional grounds that for a steady energy flux from large to small scales the kinetic energy spectrum as function of wavenumber may be presented as follows¹⁸:

$$d\mathcal{K} = \alpha_1 \varepsilon^{\alpha_2} k^{-\alpha_3} dk, \quad (10)$$

where here $k = 2\pi/\lambda$ is the wave number and λ the wavelength. ε is the dissipation rate of TKE, \mathcal{K} . Based on strict dimensional arguments, Kolmogorov [1941] proved that $\alpha_2 = 2/3$ and $\alpha_3 = 5/3$, in excellent

¹⁷It somehow resembles the “dissipative elements” discussed by the group around Norbert Peters [see Schäfer et al., 2010].

¹⁸Actually, the original arguments in Kolmogorov’s derivation were more subtle, but the use of arguments in the sense of Rayleigh’s method of dimensional analysis or, stricter, Buckingham’s π theorem, is “strict enough” for the present discussion.

agreement with the famous observations by Grant et al. [1959] in a tidal inlet with $Re \approx 10^8$ and a depth of about 100 m. A theoretically sound value of α_1 was open until today and given now below.

Devil's gear

Our view of the Kolmogorov-Richardson cascade has been changed through a study by Herrmann [1990] who has shown that Kolmogorov's value for α_3 corresponds numerically to the data of a space-filling bearing [see also Herrmann et al., 1990]. The latter is the densest non-overlapping (Apollonian) circle packing in the plane, with side condition that the circles are pointwise in contact but able to rotate freely, without friction or slipping. One may call it a "devil's gear" [Pöppe, 2004].

The contact condition for two different "wheels" with indices 1 and 2 of the gear reads

$$u = \omega_1 r_1 = \omega_2 r_2, \quad (11)$$

where u is necessarily constant throughout the gear and governed by the energy of the decaying vortex pair as $u = \sqrt{2\mathcal{K}}$. It follows that

$$\omega_2 = \omega_1 \frac{r_1}{r_2}, \quad (12)$$

so that for very small r_2 the frequency ω_2 may become acoustically relevant.

If the above gear is frictionless then the next question arises *where* – within this picture – energy could be dissipated. Clearly, in a fluid with vanishing but non-zero viscosity, dissipation happens at scales where velocity gradients are high enough, here: at a scale of measure zero. Our dissipative patch (Fig. 5 shows the first stage of its formation) is thus "almost frictionless" and therefore a Hamiltonian system, excepting scales of size zero.

The formation of a fully developed spectrum of "wheels" from Fig. 5 deserves certain perturbations "from the sides", a condition which is guaranteed by the random reconnection/recombination and scatter processes sketched in the left half of Fig. 4 and also by the incomplete mutual pressure compensation of the vortices in our vortex ensemble.

Without speculating too much we may expect that in a quasi-steady state patches like in Fig. 5 are formed via roll-up instabilities at the "surface" of the respective larger vortices. They steadily evolve into a fully developed gear. Its energy, dissipated at the smallest radii, will decrease the energy content of the primary (initial) vortex pair unless it is fed by mean flow.

The outer limits of such a patch are sketched in Fig. 6 for the begin of the cascade process. The most important message which we gain from this figure is that the *longest* or energy-containing wavelength of the dissipative patch equals $\lambda_0 = 2r$. The wavelength in a dipole is $4r$ and it forms no patch or spectrum. This difference is essential. Further below we use λ_0 as a lower integration limit for the spectral energy distribution. It is important to underline that λ_0 labels the upper wavelength limit in a dissipative patch. This limit is actually not influenced by the formation details of the spectrum.

We finally notice that the transformation of the unstable configuration of two likewise rotating vortices deserves time to set the greater masses of the smaller scales into motion. This inertia effect might play a role in highly dynamic scenarios.

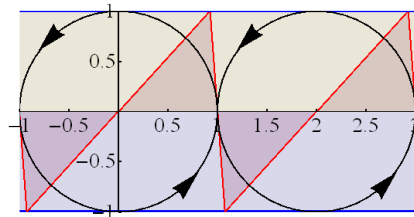


Figure 6. Outer limits of a dissipative patch (*c.f.* Fig. 5). The maximum wavelength is obviously equal to $\lambda_0 = 2r$.

7. Universal constants

In a precursor study [Baumert, 2009] it has been shown that the geometric-mechanical concept given in the present paper allows the derivation of von-Karman's constant as $\kappa = 1/\sqrt{2\pi}$. It fueled hopes that other universal constants of turbulent motion might also be derived from that apparatus.

Kolmogorov constant α_1 in the wavenumber spectrum

The TKE can be calculated by integrating (10) over the dissipative patch in the sense sketched in Figures 5 and 6 yielding

$$\mathcal{K} = \alpha_1 \varepsilon^{2/3} \int_{k_0}^{\infty} k^{-5/3} dk = \alpha_1 \frac{3}{2} \left(\frac{\varepsilon}{k_0} \right)^{2/3}, \quad (13)$$

where $k_0 = 2\pi/\lambda_0$ characterizes the lower end of the *turbulence* spectrum in the wavenumber space. We loosely assign the wavenumber range $k = 0 \dots k_0$ to the

mean flow which may basically be resolved in numerical models.

The dissipation rate ε in (13) can be expressed as follows,

$$\varepsilon = \mathcal{K}/\tau, \quad (14)$$

with τ being the lifetime of a dissipative patch. Inserting (14) in (13) and rearranging gives the following:

$$\alpha_1 = \frac{2}{3} (2\pi)^{2/3} \mathcal{K}^{1/3} \left(\frac{\tau}{2r}\right)^{2/3}. \quad (15)$$

Here we took from Fig. 6 that the energy-containing initial or primary wavelength of a dissipative patch is given by $\lambda_0 = 2r$.

Now we make a local quasi-equilibrium assumption for conditions of extremely dense vortex packing: Our marching dipoles can occupy only those places which are simultaneously “emptied” from dissipative patches by decay. This means that the life time of a dissipative patch, $\tau = \mathcal{K}/\varepsilon$, should equal the time of “free flight” of a dipole over a distance $2r$ [cf. Baumert, 2009]:

$$\tau = \mathcal{K}/\varepsilon = 2r/u. \quad (16)$$

Here we used the scalar dipole velocity u ,

$$u = \omega r = \sqrt{2\mathcal{K}}. \quad (17)$$

After some algebra, the dimensionless pre-factor of the three-dimensional wavenumber spectrum reads as follows:

$$\alpha_1 = \frac{1}{3} (4\pi)^{2/3} = 1.802. \quad (18)$$

The corresponding value of an ideal one-dimensional spectrum is one third of the above, i.e. 0.60.

Kolmogorov constant β_1 in the frequency spectrum

The generalized form of the Lagrangian frequency spectrum of fluid turbulence is the following,

$$d\mathcal{K} = \beta_1 \varepsilon^{\beta_2} \omega^{-\beta_3} d\omega, \quad (19)$$

where ω is the angular frequency. Tennekes and Lumley [1972] derived $\beta_2 = 1$ and $\beta_3 = 2$ in a similar fashion like Kolmogorov [1941] derived α_2 and α_3 [see also McComb, 2004]. The integration of (19) from $\omega = \omega_0$ to $\omega = \infty$ gives after rearrangement and using (14) the following,

$$\beta_1 = \omega_0 \tau. \quad (20)$$

Now we take from the right part of (16) $\tau = 2r/u$, from the left part of (17) $\omega_0 = u/r$ and insert both in (20) to get finally

$$\beta_1 = \omega_0 \tau = \frac{u}{r} \frac{2r}{u} = 2. \quad (21)$$

Pre-factor in the velocity autocorrelation function

The spatial autocorrelation function $B(\rho)$ of fluctuating velocities is a special second-order case of a structure function¹⁹. With the abbreviation $\rho = |\vec{\rho}|$, it is defined as follows,

$$B(\rho) = \langle u_1(\vec{x}) \times u_2(\vec{x} + \vec{\rho}) \rangle. \quad (22)$$

Here u_1, u_2 are the (scalar) velocity components of the flow velocity \vec{u} in the direction $\vec{\rho}$ connecting the points \vec{x} and $\vec{x} + \vec{\rho}$ where the velocities u_1 and u_2 are taken respectively:

$$u_1 = \vec{u}(\vec{x}) \cdot \vec{\rho}/\rho, \quad (23)$$

$$u_2 = \vec{u}(\vec{x} + \vec{\rho}) \cdot \vec{\rho}/\rho. \quad (24)$$

The central dot denotes the scalar product (or dot product). Notice that, rather than a density, ρ is here a spatial distance.

In their §34 on p. 145 Landau and Lifshitz [1987] have shown that, based on early results by Kolmogorov, $B(r)$ in (22) may be written as follows,

$$B(r) = C \times (\varepsilon \rho)^{2/3}, \quad (25)$$

where C is a dimensionless numerical constant which is related with α_1 from the universal wavenumber spectrum (10) as follows,

$$C = \alpha_1 \frac{27}{55} \Gamma(1/3) \quad (26)$$

$$= \frac{1}{3} (4\pi)^{2/3} \frac{27}{55} \Gamma(1/3) \quad (27)$$

$$\approx 2.37. \quad (28)$$

Here $\Gamma(z)$ is the Euler gamma function.

In contrast to our derivations of κ , α_1 and β_1 the value (28) for C should be taken with care because the derivation of its relation with α_1 by Landau and Lifshitz uses an *approximation* and is thus valid for small values of the distance variable ρ only, i.e. for $\ll \lambda_0 = 2\bar{r}$.

8. Discussion

Comparison with observations

The rounded numerical values $\kappa = 0.4$, $\alpha_1 = 1.8$, $\alpha_1/3 = 0.6$, and $\beta_1 = 2$ for von Karman’s and Kolmogorov’s universal constants predicted by our theory are situated well within the error bars of many high-*Re*

¹⁹For details see §34 in Landau and Lifshitz [1987].

number observations, NSE and RG based analytical approximations, laboratory and DNS experiments. Based on observations, Tennekes and Lumley [1972] gave the values $\alpha_1 = 1.62$ and $\beta_1 = 2.02$, but with greater uncertainty.

Later works have been analysed in an important study by Sreenivasan [1995] who possibly gave the most comprehensive literature review of experimental and observational values for the number $\alpha_1/3$ until now. Later Yeung and Zhou [1997] reported a value of $\alpha_1 = 1.62$ based on high-resolution DNS studies with up to 512^3 grid points.

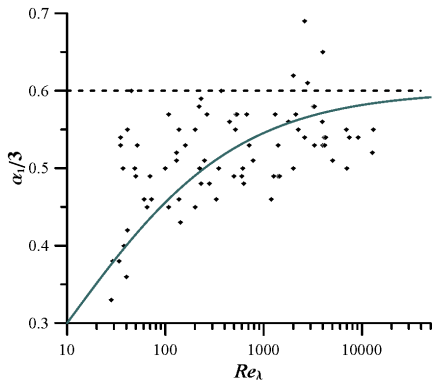


Figure 7. Experimental and observational results for $\alpha_1/3$ measured, collected from the literature, and analysed by Sreenivasan [1995]. The solid green line follows our somewhat arbitrary approximation $0.6 \times \sqrt{Re_\lambda} / (\sqrt{Re_\lambda} + \sqrt{Re_*})$ wherein $\alpha_1/3 = 0.6$ is the theoretically derived asymptotic value. Here we took $Re_* = 10$. A similar presentation has been chosen by Sreenivasan [1995] for $\alpha_1/3$ in his Fig. 3, and by Yeung et al. [2006] for $\pi\beta_1$ in their Fig. 2.

The results of their later efforts suggest, again with DNS but based on a grid of 2048^3 points, the value $\beta_1 = 2.1$ [Yeung et al., 2006, their Fig. 3]. In a recent study by Donzis and Sreenivasan [2010] a DNS grid of 4096^3 has led to $\alpha_1 \approx 1.58$.

Based on their oceanic measurements (with much higher Reynolds numbers compared with DNS) Lien and D’Asaro [2002] found that $\beta_1 = 1.75 \dots 2.04$. They state that

... since the present uncertainty is comparable to that between high quality estimates of the Eulerian one-dimensional longitudinal Kolmogorov constant measured by many dozen investigators over the last 50 years, large improvements in the accuracy

of the estimate of β_1 seem unlikely.

Beginning with an initiating work by Forster et al. [1977], systematic analytical approximations using RG methods and related techniques for NSE became further sources of estimates for the universal constants. E.g. Yakhot and Orszag [1986b, a] reported $\alpha_1 \approx 1.62$ whereas McComb and Watt [1992] derived $\alpha_1 = 1.60 \pm 0.01$ and Park and Deem [2003] obtained $\alpha_1 = 1.68$. We note that these approximations are technically extremely complex and neither unique nor part of an integrated descriptive concept for turbulence.

Turbulence plays a crucial role in almost all fields of engineering, including medical applications, and in geophysical fluid dynamics up to climate-change studies. It plays an essential part in our everyday life. When we leave our house or ride our bike, when we jump into our pool – we always are literally embedded in a turbulent fluid. Compared with most other fields of modern physics the present scatter in the values of the universal constants is uniquely high and therefore actually not longer acceptable. However, our theoretical results containing irrational and transcendental numbers suggest that the universal constants of turbulence *can principally not be measured* in real-world fluids. Or would *measuring π* be a reasonable task?

A possible solution of this dilemma is the asymptotic analysis of measurements at higher and higher Reynolds numbers so that an extrapolation to $Re \rightarrow \infty$ becomes feasible with some certainty. The data analyses by Sreenivasan [1995] and the report by Yeung et al. [2006] could serve as a methodical model. Fig. 7 shows a re-plot of Sreenivasan’s data with Re on the abscissa and measured $\alpha_1/3$ on the ordinate. The data exhibit a visible tendency to grow with increasing Re to a saturation value which is statistically indistinguishable from our 0.6.

Universality and fundamentality; turbulence, physics, and geometry

Besides problems and tasks posed in engineering and geophysical fluid dynamics where prediction accuracy and extrapolability matter most, there is a question posed by natural philosophy: how are universal constants of turbulent motion, fundamental physics constants like the electron’s elementary charge [see e.g. Fritzsche, 2009], and mathematical constants like π related with each other?

First, the measurement accuracy of “turbulent numbers” is *extremely poor*.

Second, “turbulent constants” characterize universal

properties of a *specific* (turbulent) form of dynamic and self-similar *motions* rather than more “static” properties like the elementary charge. They are thus closer to the vacuum speed of light or the Hubble constant describing the (accelerated) expansion motion of the universe.

Third, like mathematical constants, “turbulent numbers” are dimensionless whereas fundamental physics motion constants like the Hubble or the vacuum speed of light are given in kilometers per second. The latter are absolute values. “Our” constants characterize self-similar motions²⁰.

This provokes the question whether geometry is part of physics or vice versa, as discussed for instance by Palais [1981]. One might argue that the discovery of the constant angle sum in triangles was historically the first discovery of a physical conservation law by man, made and explicitly formulated much earlier than the conservation laws of volume, mass etc.²¹

The completed image of turbulent flows

For the sake of clarity we concentrate on the most simple non-trivial situation, a spatially one-dimensional channel flow with velocity component U in horizontal (x) direction, with vertical variation along z , and with horizontal, \tilde{u} , and vertical velocity fluctuations, \tilde{w} . An example of this situation has been presented earlier [see eq. (4.20) and (4.21) in Baumert, 2005a, where stratification is already considered through the squared buoyancy frequency, N^2]. The Reynolds decomposition of our flow field then reads as follows:

$$U(z, t) = \langle U \rangle + \tilde{u}(z, t), \quad (29)$$

$$W(z, t) = \langle W \rangle + \tilde{w}(z, t). \quad (30)$$

Mean flow: RANS. One may now insert (29, 30) into the corresponding two-dimensional Euler equation to find together with mass conservation the following,

$$\frac{\partial \langle U \rangle}{\partial t} + \frac{\partial \langle \tilde{u} \tilde{w} \rangle}{\partial z} = - \frac{\partial \langle p \rangle}{\partial x}, \quad (31)$$

²⁰ If we exclude from our consideration physical cosmology and arbitrarily chosen ratios between masses of the various atoms and molecules then physics has actually only one dimensionless exception: Sommerfeld’s fine-structure constant, with a value of about 137. Wolfgang Pauli has long been preoccupied with the question of why, and Richard Feynman [1985] even speculated about a relation with π . Here we have shown that π is at least related with constants of turbulent motion.

²¹ These thoughts are actually outside the scope of the present report. Some patience is needed as a “theory of everything” is not in sight [Laughlin, 2005], and just-answered questions typically give birth to new conundrums.

where $\langle p \rangle$ is the pressure. Equation (31) is usually called a Reynolds-averaged Navier-Stokes equation (RANS). Here we take the case of vanishing molecular viscosity.

Turbulent mixing: downgradient flux. Equation (31) is not yet closed because the correlator describing a diffusive flux, $\langle \tilde{u} \tilde{w} \rangle$, needs to be specified, a task which consumed substantial efforts over the last 60 years. The following quasi-linear flux-gradient relation is theoretically well established in many branches of many-particle physics and reads in our case as follows:

$$- \langle \tilde{u} \tilde{w} \rangle = \nu \frac{\partial}{\partial z} \langle U \rangle. \quad (32)$$

Kolmogorov-Prandtl relation. However, also (32) does not yet close the problem because now the so-called turbulent viscosity, ν , needs to be specified. In our picture the latter is again presented in a many-particle format in analogy to Einstein’s theory of Brownian motion as follows [for details see Baumert, 2009]:

$$\nu = L^2 / \tau = \mathcal{K} / (\pi \Omega). \quad (33)$$

Here $L = r / \kappa$ and $\tau = 1 / \Omega$ are locally averaged²² space and time scales which are expressed within the framework of our mechanistic dipol-chaos model in terms of \mathcal{K} and $\omega = 2 \pi \Omega$.

Equations of turbulent motion, neutral stratification. We skip here the technical details of derivations given in Baumert [2009] and quote only the result that the variables \mathcal{K} and Ω are governed by a specific system of nonlinear partial differential equations as follows:

$$\frac{\partial \mathcal{K}}{\partial t} - \frac{\partial}{\partial z} \left(\nu \frac{\partial \mathcal{K}}{\partial z} \right) = \nu \left[\left(\frac{\partial \langle U \rangle}{\partial z} \right)^2 - \Omega^2 \right], \quad (34)$$

$$\frac{\partial \Omega}{\partial t} - \frac{\partial}{\partial z} \left(\nu \frac{\partial \Omega}{\partial z} \right) = \frac{1}{\pi} \left[\frac{1}{2} \left(\frac{\partial \langle U \rangle}{\partial z} \right)^2 - \Omega^2 \right] \quad (35)$$

These equations resemble at least the structure of the so-called \mathcal{K} - Ω closure model used by many authors [loc. cit. Wilcox, 2006]. They use differing empirically gained sets of prefactors of the terms and cannot identify the physical nature of Ω . Our derivation of (34, 35) should not be confused with a new “scheme” or closure of this sort because – as we have shown – our equations are founded solidly on the most simple principles of hydrodynamics and many-particle physics, without use of phenomenological data and, for the first time, giving even the universal constants of turbulent motion. On

²²For reasons of transparency the overbars are omitted.

the other hand, the experience of Wilcox [2006] and colleagues shows that practical experiments and application needs guide the creative engineer very close to the physically correct solution, of course, without guiding further to the universal constants.

Turbulence spectra. With the dissipation rate ε ,

$$\varepsilon = \mathcal{K} \Omega / \pi, \quad (36)$$

we may express the spectra in the admissible turbulent ranges $k = k_0 \dots \infty$ and $\omega = \omega_0 \dots \infty$ as follows:

$$\frac{d\mathcal{K}}{dk} = \alpha_1 \varepsilon^{2/3} k^{-5/3}, \quad (37)$$

$$\frac{d\mathcal{K}}{d\omega} = \beta_1 \varepsilon \omega^{-2}, \quad (38)$$

where turbulence begins at

$$k_0 = \pi / \kappa L = \pi^2 \Omega \sqrt{2/\mathcal{K}}, \quad (39)$$

$$\omega_0 = \Omega / \kappa^2 = 2\pi \Omega, \quad (40)$$

respectively. Longer scales or slower motions are possibly turbulent, but not in the sense of a fully developed spectrum. In the case of slow variations of the driving forces the motions outside the validity range belong to the mean flow. Notice that the lower limits of the turbulent spectral ranges are *dynamic* quantities which are controlled by the dynamic variables \mathcal{K} and Ω .

Universal constants. The values of our theoretically derived universal constants of turbulent motion are

$$\alpha_1 = \frac{1}{3} (4\pi)^{2/3} = 1.802, \quad (41)$$

$$\beta_1 = 2, \quad (42)$$

$$\kappa = 1/\sqrt{2\pi} = 0.399. \quad (43)$$

Solid boundaries. TKE cannot penetrate solid boundaries like walls, which is sometimes called an ‘adiabatic boundary condition’, in analogy to heat conduction. Assuming the wall at $z = z_*$ this means that the following condition has to be satisfied:

$$\left. \frac{\partial \mathcal{K}}{\partial z} \right|_{z=z_*} = 0. \quad (44)$$

This is already sufficient to solve (34, 35) at solid walls and produce the logarithmic law of the wall. A second condition for Ω is not needed due to the a.m. nonlinearities of the equations [for details see Baumert, 2005a].

Stable stratification. Stable stratification may be described by the following modification of (34):

$$\frac{\partial \mathcal{K}}{\partial t} - \frac{\partial}{\partial z} \left(\nu \frac{\partial \mathcal{K}}{\partial z} \right) = \nu \left[\left(\frac{\partial \langle U \rangle}{\partial z} \right)^2 - 2N^2 - \Omega^2 \right]. \quad (45)$$

This description is valid as long as $\Omega \geq N$. In the case of free decay and linear stratification, Ω approaches N ‘from above’. Due to the dispersion relation for internal waves, slow disordered turbulent motions at $\Omega \approx N$ and slower can only exist as waves so that turbulence is converted into internal waves when $\Omega \rightarrow N$. The stratification aspects are discussed by Baumert and Peters [2004, 2005] in greater detail and in relation to observations and measurements.

Limitations. A trivial limitation for (45) is $N^2 \geq 0$. For unstable or convective situations these equations are possibly not applicable, but we did not yet test this case.

Equations (29 – 44) form a closed, complete description of mean and turbulent motions, including their wavenumber and frequency spectra with their universal spectral constants, applicable under neutrally stratified conditions. For stably stratified flows (34) needs to be replaced with (45), provided that there are *no* external sources of internal-wave energy. This means that, due to the ubiquitous presence of internal waves in most geophysical flows, the latter are *not* covered by (45). Some modifications are necessary and a certain knowledge of the sources of internal-wave energy is needed. The necessary modifications are not part of this report.

The difference between (34, 35) or (45, 35) on the one hand, and traditional phenomenologically based closure schemes discussed e.g. by Wilcox [2006] on the other, is mathematically minimal but physically relevant. Those schemes use for instance quantities like ε or τ as primary variables in balance equations although conservation laws for those quantities do not exist. The differences are becoming generally relevant and visible at solid boundaries and, in the stratified case, also within the turbulent fluid volume.

An important limitation has already been mentioned above. Further, variations in the mean flow field should be relatively slow and spatial gradients not too strong so that we may talk about time-dependent but quasi-steady behavior with sufficiently homogeneous state variables on local scales and sufficiently developed Kolmogorov spectra. This excludes shock-waves from our considerations. But also this limitation has not been tested yet.

The free decay of turbulence might be such a case. Our theory predicts the decay of TKE to scale with t^{-1} [or with $(x/U)^{-1}$ in the wind tunnel]. This is also supported through a group-theoretical analysis by Oberlack [2002]. Whereas wind-tunnel data [Batchelor, 1953] and selected free-decay measurements [Dickey and Mellor, 1980] agree surprisingly well with our theory, in

some experiments if rapid free decay the exponent is somewhat greater than unity. This situation is challenging and needs a further study.

We may summarize as follows:

- The present theory is based on conservation laws and geometry only, without use of empirical data.
- Besides spectrally integrated parameters like turbulent viscosity, dissipation rate etc., it gives full turbulent spectra, even under non-stationary conditions.
- The theory predicts fundamental constants of turbulent motion.
- The approach is limited to slow and smooth mean flows under neutral or stable stratification.
- Internal gravity waves are taken into account only so far as they are intrinsically coupled with local current shear.

Our methodology differs from past concepts. The latter use specific series expansions of the Navier-Stokes equation into a system of partial differential equations for higher and higher moments in the perturbations, with the zeroth hierarchy element being the Reynolds equation (RANS). The k - ε , the Mellor-Yamada, k - τ , the k - ω and the many other turbulence-closure schemes populating the literature are examples [e.g. Baumert et al., 2005; Wilcox, 2006].

The present picture includes a perturbation step, too, but it stops at the zeroth level, at RANS. Here the turbulent fluxes still remain unknown. We then took into account that each fluid element experiences an effective total force field consisting additively of the external mean field $\bar{\mathcal{H}}$ acting in the total fluid volume, and of the field $\tilde{\mathcal{H}}$ controlled by nearest neighboring vortex dipoles (“Ising assumption”),

$$\mathcal{H} = \bar{\mathcal{H}} + \tilde{\mathcal{H}}. \quad (46)$$

Our results show that $\tilde{\mathcal{H}}$ is locally best described by a simple white-noise stochastic force. This approach has successfully been used about 100 years ago by Langevin, Smoluchowsky and Einstein in theoretical analyses of Brownian motion. This assumption directly delivers Fokker-Planck equations for the expectation-value distribution functions of particle number and of particle properties \mathcal{K} and Ω .

The theory applies exclusively to locally homogeneous, locally isotropic and weakly unsteady turbulent

flows. To extreme non-stationarities and/or sharp spatial gradients like in shockwaves it is possibly not applicable. As a rule, temporal changes of the mean flow should take place on time scales sufficiently greater than $1/\Omega$ because otherwise the Kolmogorov spectra (37, 38) are not yet well enough established.

Coda. The theory completed here will hopefully not form a Procrustean bed in Saffman’s (1977) sense [loc. cit. Davidson, 2004, p. 107] who even feared that “in searching for a theory of turbulence, perhaps we are looking for a chimera ...”. This view has just recently been enforced by Hunt [2011] as follows: “But there are good reasons why the answer to the big question that Landau and Batchelor raised about whether there is a general theory of turbulence is probably ‘no’.”

As the above smacks of defeatism, we pass the word to Sir Winston Churchill who demanded in a critical situation “We shall never surrender!” He surely would encourage a new generation of men and women to follow their own fresh ideas towards a general theory of turbulence at asymptotically high Reynolds numbers.

Acknowledgments. This report profited substantially from the scientific cooperation between the author and Hartmut Peters at Earth and Space Research in Seattle, WA, who even contributed Figures 1 to 3, and major paragraphs of Chapter 3 of the present report. The cooperation took place within the framework of the Department of the Navy Grant N62909-10-1-7050 issued by the Office of Naval Research Global. The United States Government has a royalty-free license throughout the world in all copy-rightable material contained herein.

The author is thankful to Eckhard Kleine who directed the attention to the remarkable works of Hans J. Herrmann and helped as a robust sparring partner in turbulent debates. Special thanks are due to Stephen A. Thorpe who critically commented the precursor version of this report. Thanks are further due to David I. Benjamin, Peter Braun, Eric D’Asaro, Bruno Eckhardt, Philippe Fraunier, Harald Fritzsche, Boris Galperin, Rupert Klein, Ren-Chieh Lien, Jim Riley, Gisbert Stoyan, John Simpson, Jürgen Sündermann, Oleg F. Vasiliev, Michael Wilczek, and Sergej S. Zilitinkevich.

The author thanks particularly the conference organizers of *Turbulent Mixing and Beyond 2011* at the Abdus Salam International Centre of Theoretical Physics, Trieste/Italy, where the above text has been presented for the first time. Special thanks are due to Snezhana Abarzhi and Joseph J. Niemela who managed to create a fair, open and creative scientific atmosphere.

References

- Albring, W., 1981: *Elementarvorgänge fluider Wirbelbewegungen*. Akademie-Verlag, 302 pp.
- Anderson, P. W., 1972: More is different. *Science*, **177**, 393 – 396.
- Batchelor, G. K., 1953: *The theory of homogeneous turbulence*. Cambridge University Press, 197 ff. pp.
- Baumert, H., J. Simpson, and J. Sündermann, 2005: *Marine Turbulence*. Cambridge University Press, 640 pp.
- Baumert, H. Z.: 2005a, A novel two-equation turbulence closure for high Reynolds numbers. Part B: Spatially non-uniform conditions. *Marine Turbulence: Theories, Observations and Models*, H. Z. Baumert, J. H. Simpson, and J. Sündermann, eds., Cambridge University Press, Chapter 4, 31 – 43.
- 2005b, On some analogies between high-Reynolds number turbulence and a vortex gas for a simple flow configuration. *Marine Turbulence: Theories, Observations and Models*, H. Z. Baumert, J. H. Simpson, and J. Sündermann, eds., Cambridge University Press, Chapter 5, 44 – 52.
- Baumert, H. Z., 2009: Primitive turbulence: kinetics, Prandtl’s mixing length, and von Karman’s constant. *arXiv.org [physics.flu-dyn]*, **0907.0223v2**, 1 – 12.
- Baumert, H. Z. and H. Peters, 2004: Turbulence closure, steady state, and collapse into waves. *J. Phys. Oceanography*, **34**, 505 – 512.
- Baumert, H. Z. and H. Peters: 2005, A novel two-equation turbulence closure for high Reynolds numbers. Part A: Homogeneous, non-rotating stratified shear layers. *Marine Turbulence: Theories, Observations and Models*, H. Z. Baumert, J. H. Simpson, and J. Sündermann, eds., Cambridge University Press, Chapter 3, 14 – 30.
- Bertalanffy, L., 1953: *Biophysik des Fließgleichgewichts*. Vieweg, Akademie-Verlag, 2nd rev. ed. by W. Beier and R. Laue edition, 56 pp.
- Chandrasekhar, S., 1979: Beauty and the quest for beauty in science. *Physics Today*, July, 225 – 30.
- D’Asaro, E. A. and R.-C. Lien, 2000: Lagrangian measurements of waves and turbulence in stratified flows. *J. Phys. Oceanogr.*, **30**, 641 – 655.
- Davidson, P. A., 2004: *Turbulence. An introduction for scientists and engineers*. Oxford University Press, 657 pp.
- Dickey, T. D. and G. L. Mellor, 1980: Decaying turbulence in neutral and stratified fluids. *J. Fluid Mech.*, **99**, 37 – 48.
- Dillon, T. M., 1982: Vertical overturns: A comparison of Thorpe and Ozmidov length scales. *J. Geophys. Res.*, **87**, 9,601 – 9,613.
- Donzis, D. A. and K. R. Sreenivasan, 2010: The bottleneck effect and the Kolmogorov constant in isotropic turbulence. *J. Fluid Mech.*, **657**, 171 – 188.
- Dresden, M.: 1993, Renormalization in historical perspective – the first stages. *Renormalization. From Lorentz to Landau and beyond.*, L. M. Brown, ed., Springer-Verlag, 31 – 56.
- Einstein, A., 1905: Über die von der molekularkinetischen Theorie der Wärme geforderte Bewegung von in ruhenden Flüssigkeiten suspendierten Teilchen. *Annalen der Physik*, **17**, 549 – 560.
- Ellison, T. H., 1957: Turbulent transport of heat and momentum from an infinite rough plane. *J. Fluid Mech.*, **2**, 456 – 466.
- Feynman, R. P., 1963: *Six Easy Pieces: Essentials of Physics Explained by Its Most Brilliant Teacher*. Perseus Books, 209 pp.
- 1985: *QED: The Strange Theory of Light and Matter*. Princeton University Press, 129 pp.
- Forster, D., D. Nelson, and M. Stephen, 1977: Large-distance and longtime properties of a randomly stirred fluid. *Phys. Rev. A*, **16**, 732 – 749.
- Frisch, U., 1995: *Turbulence. The legacy of A. N. Kolmogorov*. Cambridge University Press, 296 pp.
- Fritzsche, H., 2009: *The fundamental constants. A mystery of physics*. World Scientific, 192 pp.
- Glansdorff, P. and I. Prigogine, 1971: *Thermodynamic theory of structure, stability and fluctuations*. John Wiley & Sons Ltd., 306 pp.
- Grant, H. L., A. Moilliet, and R. Stewart, 1959: A spectrum of turbulence at very high Reynolds number. *Nature*, **184**, 808 – 810.
- Haken, H., 1978: *Synergetics*. Springer-Verlag, 2 edition, 355 pp.
- 1983: *Advanced Synergetics*. Springer-Verlag.
- Herrmann, H. J.: 1990, Space-filling bearings. *Correlation and Connectivity*, H. E. Stanley and N. Ostrowsky, eds., Kluwer Academic Publ., 108 – 120.
- Herrmann, H. J., G. Mantica, and D. Bessis, 1990: Space-filling bearings. *Phys. Rev. Letters*, **65**, 24 December, 3,223 – 3,226.
- Hinze, J. O., 1953: *Turbulence*. McGraw-Hill Book Comp., 586 pp.
- Hunt, J., 2011: The importance and fascination of turbulence. Public Evening Lecture, Old Library, ERCOFTAC – 13th European Turbulence Conference 12-15 September 2011, Warsaw, Poland, etc13.fuw.edu.pl/speakers/public-evening-lecture.

- Imberger, J. and B. Boashash, 1986: Application of the Wigner-Ville distribution to temperature gradient microstructure: a new technique to study small-scale variations. *J. Phys. Oceanography*, **16**, 1997 – 2012.
- Itsweire, E. C., K. N. Helland, and C. W. V. Atta, 1986: The evolution of grid-generated turbulence in a stably stratified fluid. *J. Fluid Mech.*, **162**, 299 – 338.
- Keller, L. and A. Friedmann: 1924, Differentialgleichungen für die turbulente Bewegung einer inkompressiblen Flüssigkeit. *Proc. First Int. Congress Appl. Mech.*, 395 – 405.
- Kolmogorov, A. N., 1941: Dissipation of energy in locally isotropic turbulence. *Dokl. Akad. Nauk SSSR*, **32**, 16 – 18.
- Kraichnan, R. H., 1968: Small-scale structure of a scalar field convected by turbulence. *The Physics of Fluids*, **11**, 945 – 953.
- Lamb, H., 1932: *Hydrodynamics*. Cambridge University Press, 6 edition, 738 pp.
- Landau, L. D. and J. M. Lifshitz, 1987: *Fluid Mechanics*, volume 6 of *Course of Theoretical Physics*. Pergamon Press, revised second english edition, 539 pp.
- Laughlin, R., 2005: *A Different Universe: Reinventing Physics from the Bottom Down*. Basic Books, 272 pp.
- Lien, R.-C. and E. A. D’Asaro, 2002: The Kolmogorov constant for the Lagrangian velocity spectrum and structure function. *Physics of Fluids*, **14**, 4456–4459.
- Lorenz, E. N., 1960: Maximum simplification of the dynamic equations. *Tellus*, **12**, 243 – 254.
- 1963: Deterministic non-periodic flow. *J. Atmos. Sci.*, **20**, 130 – 141.
- Lugt, H. J., 1979: *Wirbelströmung in Natur und Technik*. Verlag G. Braun, 460 pp.
- Marmanis, H., 1998: The kinetic theory of point vortices. *Proc. R. Soc. London A*, **454**, 587 – 606.
- McComb, W. and A. Watt, 1992: Two-field theory of incompressible-fluid turbulence. *Phys. Rev. A*, **46**, 4,797 – 4,812.
- McComb, W. D., 2004: *Renormalization Methods*. Clarendon Press, 330 pp.
- Monin, A. S. and A. M. Yaglom, 1992: *Statisticheskaya Gidromekhanika. Teoriya Turbulentnosti. Vol. 1*. Gidrometeoizdat, 694 pp.
- Oberlack, M., 2002: On the decay exponent of isotropic turbulence. *Proc. Appl. Math. Mech. (PAMM)*, **1**, 294 – 297.
- Palais, R. S., 1981: *The geometrization of physics*. Lecture Notes in Mathematics, Inst. Math. Ntl. Tsing Hua Univ. Taiwan, 91 pp.
- Paoletti, M. S., M. E. Fisher, and D. P. Lathrop, 2010: Reconnection dynamics for quantized vortices. *Physica D*, **239**, 1,367 – 1,377.
- Park, J. and M. Deem, 2003: A statistical mechanics model of isotropic turbulence well-defined within the context of the ε expansion. *Eur. Phys. J. B*, **34**, 105 – 114.
- Peters, H., M. C. Gregg, and T. B. Sanford, 1995: Detail and scaling of turbulent overturns in the Pacific Equatorial Undercurrent. *J. Geophys. Res.*, **100**, 18,349 – 18,368.
- Pöppe, C., 2004: Das Getriebe des Teufels. *Spektrum d. Wiss.*, September, 104 – 109.
- Prandtl, L.: 1926, Bericht über neuere Turbulenzforschung. *Hydraulische Probleme. Vorträge Hydrauliktagung Göttingen 5. & 6. Juni 1925*, Wiss. Beirat VDI, ed., VDI-Verlag, Berlin, 1 – 13.
- Pullin, D. I. and P. G. Saffman, 1998: Vortex dynamics in turbulence. *Ann. Rev. Fluid Mech.*, **30**.
- Reynolds, O., 1895: On the dynamical theory of incompressible viscous fluids and the determination of the criterion. *Phil. Trans. R. Soc. London A*, **186**, 123 – 164.
- Rüedi, J.-D., A. Talamelli, H. M. Nagib, P. H. Alfredsson, and P. A. Monkewitz: 2009, CICLoPE - a large pipe facility for detailed turbulence measurements at high Reynolds number. *Progress in Turbulence III*, Springer-Verlag, volume 131 of *Springer Proceedings in Physics*, p. 73 ff.
- Saffman, P. G., 1992: *Vortex Dynamics*. Cambridge Monographs on Mechanics and Applied Mathematics, Cambridge University Press, 311 pp.
- Schäfer, P., M. Gampert, J.-H. Göbbert, D. Gottschalk, and N. Peters: 2010, Geometrical dissipation element analysis in inhomogenous turbulence. *Proceedings NIC Symposium*, 24 - 25 February, Jülich, Germany, G. Münster and D. Wolf and M. Kremer, ed.
- Seman, J. A., A. L. Henn, R. F. Shiozaki, E. R. F. Ramos, M. Caracanhas, C. C. Branco, G. Roati, M. Haque, K. M. F. Magalhães, and V. S. Baginato, 2009: Observation of stable 3-vortex/anti-vortex clusters in a super-fluid Bose-Einstein condensate. *arxiv.org/abs/0907.1584v1*, **July**, 4.
- Sommerfeld, A., 1948: *Mechanik der deformierbaren Medien*, volume 2 of *Vorlesungen über Theoretische Physik*. Geest & Portig, 2 edition.

- Sreenivasan, K., 1995: On the universality of the kolmogorov constant. *Physics of Fluids*, 2,778 – 2,784.
- Stratonovich, R. L., 1992: *Nonlinear Nonequilibrium Thermodynamics I*. Springer-Verlag, 361 pp.
- 1994: *Nonlinear Nonequilibrium Thermodynamics II*. Springer-Verlag, 223 pp.
- Taylor, G. I., 1935: Statistical theory of turbulence. i. *Proc. Roy. Soc., A*, **151**, 421 – 444.
- 1937: Mechanism of the production of small eddies from large ones. *Proc. Roy. Soc., A*, **158**, 499 – 521.
- Tennekes, H. and J. L. Lumley, 1972: *A first course in turbulence*. The MIT Press, 300 pp pp.
- Thorpe, A. A., 1977: Turbulence and mixing in a Scottish loch. *Philos. Trans. R. Soc. London A*, **286**, 125 – 181.
- Trinh, K. T., 2010: On the Karman constant. *arXiv [physics.flu-dyn]*, **1007.0605v1**, 16 pp.
- Voropayeva, O. F., 2007: A hierarchy of second- and third-order turbulence models for momentumless wakes behind axisymmetric bodies. *Matematicheskiye modelirovaniye*, **19**, 29 – 51.
- Wilcox, D. C., 2006: *Turbulence Modeling for CFD*. DCW Industries, Inc., 3rd edition, 522 pp.
- Wilczek, M., 2011: *Statistical and Numerical Investigations of Fluid Turbulence*. Ph.D. thesis, Universität Münster, Germany.
- Yakhot, V. and S. A. Orszag, 1986a: Renormalization-group analysis of turbulence. *Phys. Rev. Lett.*, **57**, 1,722 – 1,724.
- 1986b: Renormalization group analysis of turbulence. i. basic theory. *J. Sci. Comp.*, **1**, 3 – 51.
- Yeung, P. K., S. B. Pope, and B. L. Sawford, 2006: Reynolds number dependence of lagrangian statistics in large numerical simulations of isotropic turbulence. *Journal of Turbulence*, **7**, 12, doi:10.1080/14685240600868272.
- Yeung, P. K. and Y. Zhou, 1997: On the universality of the Kolmogorov constant in numerical simulations of turbulence. *ICASE Report No. 97-64*, 14 pp.
- Zee, A., 1986: *Fearful symmetry. The search for beauty in modern physics*. MacMillan Publ. Comp., 356 pp.

H. Z. Baumert, IAMARIS, Bei den Mühren 69A,
D-20457 Hamburg, Germany (baumert@iamaris.org)